Brazilian Journal of Physics
ISSN: 0103-9733
luizno.bjp@gmail.com
Sociedade Brasileira de Física
Brasil

Ansari, R.; Rouhi, S.; Ajori, S.
On the Interfacial Properties of Polymers/Functionalized Single-Walled Carbon Nanotubes
Brazilian Journal of Physics, vol. 46, núm. 3, 2016, pp. 361-369
Sociedade Brasileira de Física
São Paulo, Brasil

Available in: http://www.redalyc.org/articulo.oa?id=46445584016

How to cite
Complete issue
More information about this article
Journal's homepage in redalyc.org

redalyc.org
Scientific Information System
Network of Scientific Journals from Latin America, the Caribbean, Spain and Portugal
Non-profit academic project, developed under the open access initiative

Braz J Phys (2016) 46:361–369
DOI 10.1007/s13538-016-0410-y

SOCIEDADE BRASILEIRA DE FÍSICA

ATOMIC PHYSICS

On the Interfacial Properties of Polymers/Functionalized Single-Walled Carbon Nanotubes

R. Ansari[1] · **S. Rouhi**[2] · **S. Ajori**[1]

Received: 20 August 2015 / Published online: 1 March 2016
© Sociedade Brasileira de Física 2016

Abstract Molecular dynamics (MD) simulations is used to study the adsorption of polyethylene (PE) and poly(ethylene oxide) (PEO) on the functionalized single-walled carbon nanotubes (SWCNTs). The effects of functionalization factor weight percent on the interaction energies of polymer chains with nanotubes are studied. Besides, the influences of different functionalization factors on the SWCNT/polymer interactions are investigated. It is shown that for both types of polymer chains, the largest interaction energies associates with the random O functionalized nanotubes. Besides, increasing temperature results in increasing the nanotube/polymer interaction energy. Considering the final shapes of adsorbed polymer chains on the SWCNTs, it is observed that the adsorbed conformations of PE chains are more contracted than those of PEO chains.

Keywords Nanostructures · Polymers · Molecular dynamics · Adsorption

1 Introduction

Due to remarkable mechanical, thermal, and electronic properties of carbon nanotubes (CNTs) [1–3], they are considered as good candidates for polymer matrix reinforcement to enhance their mechanical [4–6], electrical [7, 8], thermal [9, 10], and optical [11] properties. However, the difficulty in uniform dispersion of CNTs in polymer matrices limits this applicability. This drawback is related to the bundling of CNTs which is caused by van der Waals (vdW) interactions between walls of nanotubes. To overcome this difficulty, different approaches including covalent and noncovalent functionalization of CNTs have been utilized.

Rosca et al. [12] studied the effects of acid concentration, temperature, and oxidation duration on the oxidation of multi-walled CNTs (MWCNTs) in nitric acid by sample weight, Raman spectrum, solubility, morphology, and alignment. They revealed that in addition to functional groups on the MWCNT, functionalized amorphous carbon generated during the digestion of the nanotubes also affects the solubility. Osswald et al. [13] used in situ Raman experiments to monitor the structural changes in MWCNTs upon oxidation. They showed that the formation of defects and functional groups on MWCNTs can be controlled by in situ Raman spectroscopy. Datsyuk [14] investigated the influence of oxidation on the structural integrity of MWCNTs. They discussed the controlling possibility of the functionality. It was observed that the defect population/formation on the CNTs is increased by oxidation with nitric acid.

Scheibe et al. [15] quantified the functional groups formed on the surface of oxidized MWCNTs. They clarified that reduction via NaBH4 is an efficient tool to prepare MWCNTs with high hydroxyl group content from oxidized MWCNTs. The adsorption of 1-naphthylamine, 1-naphthol, and phenol on as-prepared and oxidized MWCNTs was studied by Sheng et al. [16]. They observed that 1-naphthylamine, 1-naphthol, and phenol are adsorbed spontaneously and thermodynamically favorable on the MWCNTs. Wepasnick et al. [17] explored the effects of six commonly used wet chemical oxidants including HNO3, KMnO4, H2SO4/HNO3,

✉ S. Rouhi
s_rouhi@iaul.ac.ir

[1] Department of Mechanical Engineering, University of Guilan, P.O. Box 3756, Rasht, Iran

[2] Young Researchers and Elite Club, Langroud Branch, Islamic Azad University, Langroud, Guilan, Iran

(NH4)2S2O8, H2O2 and O3 on the surface chemistry and structure of MWCNTs. It was observed that the distribution of oxygen-containing functional groups is not affected by the reaction conditions (e.g., *w*/*w*% of oxidant), but depends on the identity of the oxidant.

Chiang et al. [18] studied the variation of MWCNTs nature due to different degrees of oxidation. They proposed the oxidation mechanism of MWCNTs in mild H2SO4/HNO3 mixture as a good oxidation mechanism. Andrade et al. [19] evaluated the effects of temperature on the nitric acid oxidation MWCNTs. Based on their results, the generation of oxidized industrial grade MWCNTs is strongly depends on the temperature. Pandey et al. [20] established an approach for wet mechanochemical oxidation CNTs to reach a uniform nanodispersion of the CNTs. They observed that the mechanical properties of nanocomposites reinforced with wet mechanochemically oxidized CNT (McCNT) are better than those of acid-oxidized CNTs. In addition to the mentioned experimental approaches, some simulations have also been performed in this field. A survey on the CNTs decorated by different atoms using quantum chemical and molecular dynamics is given in [21].

Besides, numerous experimental [22–32] and simulation [33–43] works are conducted to study the noncovalent functionalization of CNTs. Foroutan and Nasrabadi studied the interaction between SWCNTs and polythiophene (PT), polypyrrole (PP), poly(2,6-pyridinylenevinylene- co −2,5-dioctyloxy- p-phenylenevinylene) (PPyPV), and poly(m-phenyl-enevinylene-co −2,5-dioctyloxy- p-phenylenevinylene) (PmPV). Based on their results, it was observed that in a polymer/CNT system, the structure of polymer chain and nanotube radius strongly affects the intermolecular interaction [35].

Tallury and Pasquinelli studied the interfacial properties of SWCNTs and polymer chains with flexible [36] and semiflexible and stiff backbones [37]. They observed more distinct conformations in the wrapping of polymer chains with stiff and semiflexible backbones. The interactions between cyclodextrins (CDs) and CNTs were studied by Pang et al. [38]. Based on their results, it was revealed that the structures of CDs such as substituted group and position strongly affect the conformation of polymer chain adsorbed on the CNT surface.

Rouhi et al. [41] studied the influences of different factors such as SWCNT geometry, temperature, and polymer chain length on the PE/SWCNT interactions. They also studied the adsorption of poly(phenylacetylene), polystyrene sulfonate, and polyvinyl pyrrolidone on the surface of SWCNTs [42]. They showed that the effect of temperature on the polymer/nanotube interaction energy is small. Jilili et al. [43] used first-principles calculations to investigate the binding of poly[(9,9-bis-(6-bromohexylfluorene-2,7-diyl)-co-(benzene-1,4-diyl)] to SWCNT and graphene. They showed that conjugated polymer can be used for noncovalent functionalization.

In this article, using MD simulations, the adsorption of PE and PEO chains on functionalized SWCNTs are investigated. As it was previously mentioned, both covalent and noncovalent functionalizations have been used to improve the applicability of CNTs in nanotube reinforced polymers. To the authors' knowledge, in all of the aforementioned papers, only one of covalent and noncovalent functionalizations has been considered. Herein, the effect of employing the covalent and noncovalent functionalizations simultaneously on polymer/SWCNT interaction is investigated. The results can be useful in nanocomposite manufacturing for improvement of nanotube dispersion and better transfer of nanotube properties to the surrounded matrix. The effect of different factors such as functionalization factor type and weight percent on the polymer/functionalized SWCNT interactions are studied. Besides, a commonly used simplification in the studying of polymer chain adsorption in the SWCNTs, in which the SWCNT atoms are frozen during simulation, is investigated.

2 Details of MD Simulations

LAMMPS MD code [44, 45] is utilized to perform MD simulations. All of the simulations are done under the NVT (constant number of molecules, constant volume, and constant temperature) ensemble with the constant temperature of 300 K. Besides, Nose–Hoover thermostat algorithm is employed for simulations and velocity Verlet algorithm [46] is used to integrate the equations of motion. The timesteps and cutoff distances are considered as 1 fs and 10 Å. All of the interactions are modeled by using the AMBER force field [47] which is found to be a reliable force field in similar systems [48–50]. The simulations have performed for 250 ps. The periodic boundary conditions are applied in all of the directions.

Based on the selected number of atoms of polymer chains, the number of repeat units is computed. Then, the polymer chains are constructed by putting these repeat units at the side of each other. The functionalized CNTs are built by a MATLAB code. Based on the chirality and length, the SWCNT are built and then, the functionalization factors are dispersed along the length of the nanotubes. Accordingly, the functionalized CNTs and the chains located perpendicular to the SWCNT axis are prepared by a self-developed MATLAB code.

Moreover, all of the simulations were performed at the constant temperature of 300 K. Noted that whole structures are initially minimized and relaxed, separately, in selected ensemble to reach their equilibrated structure, then polymers are located near the functionalized CNTs. Also, each simulation runs for three times and the average of calculated parameters are reported.

3 Molecular Model

3.1 Functionalized SWCNTs

Herein, CNTs are functionalized with atomic oxygen and hydroxyl (O-H) groups known as functionalized factors [51]. To this end, a (7,7) CNT with length of 110 Å is selected and components are chemisorbed chemically on its surface with different patterns and weight percentages (functionalized factor). The weight percentage is defined as the ratio of the mass of the attached functional group to the whole mass of CNT. To demonstrate this, Fig. 1I, II is revealed. As illustrated, there are two distribution patterns for both chemisorbed components, i.e. mapped and random, abbreviated by MO, MOH, ROROH, RO and ROH which are explained as regular pattern distribution of oxygen atoms, regular pattern distribution of O-H (−hydroxyl), random pattern distribution of combination of oxygen atoms and O-H (−hydroxyl), random pattern distribution of oxygen atoms and random pattern distribution of O-H (−hydroxyl), respectively. Initial relaxation process shows that according to chemisorption component, the cross section of CNT changes considerably. This is depicted in Fig. 1III. As shown, circular shape of CNT cross section is altered to polygons with sharp corners at the site of hydroxyl chemisorption, whereas atomic oxygen chemisorption changes the cross section of CNT to oval-like shape or any noncircular soft corner shapes. It should be noted that in some models of functionalized CNTs with mapped distribution pattern, initial curvature is initiated in the CNT. Also, it is observed that in the models with random distribution patterns the circular shape of CNT is almost preserved, whereas the diameter rises slightly to its equilibrium value which is small enough and can be neglected.

I.

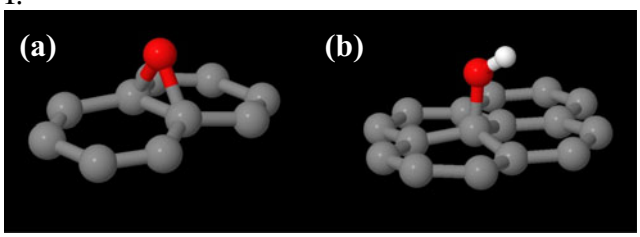

II.

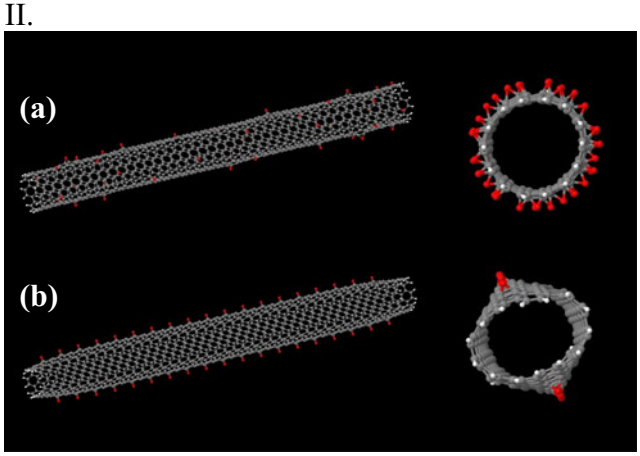

III.

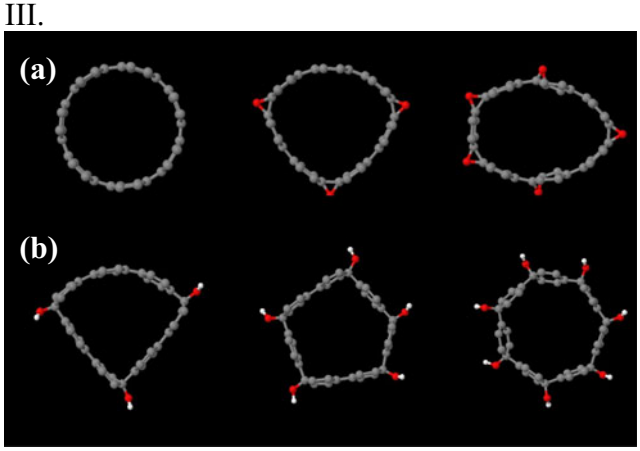

Fig. 1 *I* Chemisorption of (*a*) atomic oxygen, (*b*) hydroxyl, *II* Schematic of distribution pattern (*a*) random, (*b*) mapped. *III* Cross section change of functionalized CNTs

3.2 Polymer Chains

The PE and PEO chains are selected to study their adsorption on the SWCNT surface. The polymer chains repeating units are shown in Fig. 2. PE chains are selected with 100 monomers which contain 602 atoms including 200 C and 402 H atoms. Besides, PEO chains having 86 monomers mean 172 C, 86 O, and 346 H atoms. As it can be seen, the number of atoms are approximately equal. It should be noted that, as the results of physical adsorption of polymers on CNTs are insensitive to the initial configuration of the simulations models, the polymers, initially, are located parallel to the axis of functionalized CNTs.

4 Results

The adsorption energy of the polymer/nanotube system is obtained as

$$E_{\text{inter}} = E_{\text{polymer-CNT}} - \left(E_{\text{polymer}} + E_{\text{CNT}}\right) \quad (1)$$

in which E_{inter} is the interaction energy and $E_{\text{polymer-CNT}}$, E_{polymer} and E_{CNT} are the potential energies of polymer/nanotube system, polymer and nanotube, respectively.

PE PEO

Fig. 2 Repeat units of polymer chains

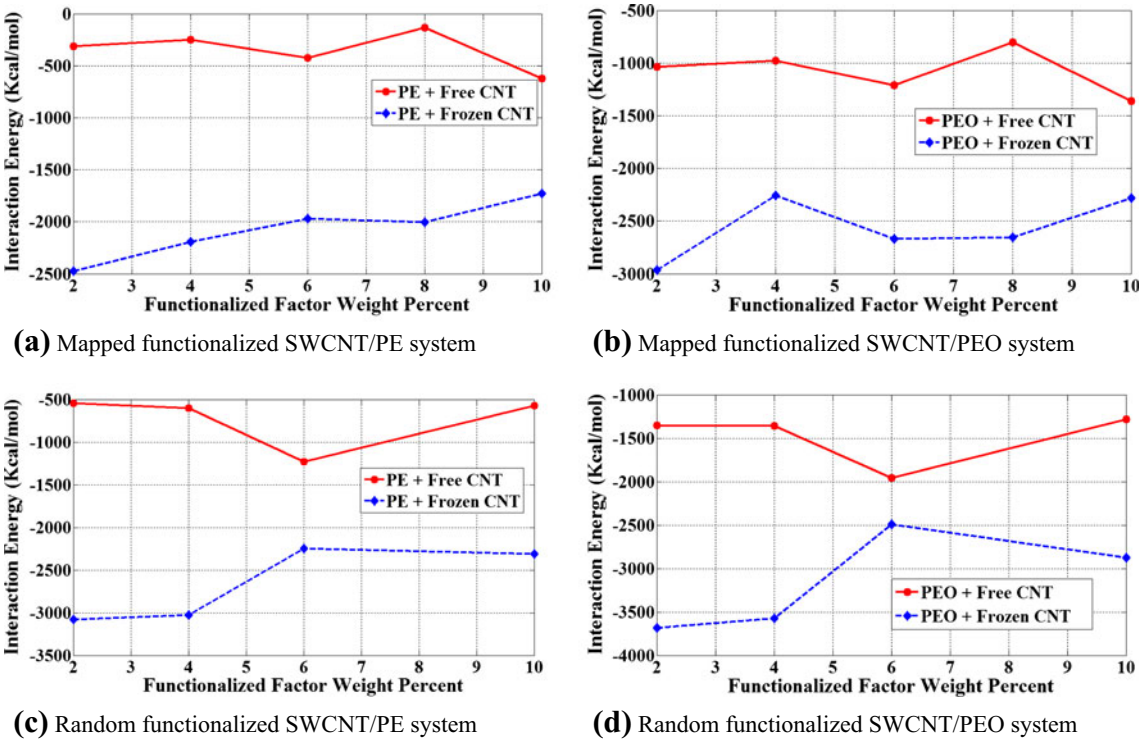

(a) Mapped functionalized SWCNT/PE system

(b) Mapped functionalized SWCNT/PEO system

(c) Random functionalized SWCNT/PE system

(d) Random functionalized SWCNT/PEO system

Fig. 3 Comparison of the interaction energies of polymer chains with free and frozen O functionalized SWCNTs.

It has been observed that during simulation, the change of pure SWCNT without functionalization can be neglected. So, to decrease the computation time, different researchers have fixed all of the nanotube atoms, meaning that the SWCNT is frozen [30, 36, 37, 41, 52]. To investigate this property for functionalized SWCNT, the adsorption of PE and PEO polymer chains is studied for free and frozen nanotubes. The results for mapped and random O functionalized SWCNTs are given in Fig. 3.

It is observed that, generally, the difference between interaction energies of polymer chains with free and frozen SWCNT is large and cannot be neglected. For both of the considered chains, the interaction of polymer chain with free functionalized SWCNTs is less powerful than that in the frozen SWCNT/polymer systems.

A similar trend is observed for both of the chains. Besides, by comparing the graphs associated with mapped and random functionalized SWCNTs (a and c, b and d), one can conclude that for free and frozen SWCNTs, the systems containing random functionalized nanotubes have larger interaction energies with polymers as compared to mapped functionalized SWCNTs. Other types of functionalization lead to same results.

In Table 1, the interaction energies of PE chain/different functionalized SWCNTs are compared with those reported in [41] for PE chain/unfunctionalized SWCNTs. According to this table, one can observe that functionalizing SWCNTs by different weight percentages of O factors can decrease the interaction energies. However, OH factor increases the polymer/SWCNT interaction energies. So, it can be used to enhance the strength polymer/nanotube interface which in turn promotes the mechanical properties of SWCNT reinforced polymers. For random mixed functionalized SWCNT, both decrease and increase occur.

In Figs. 4, 5, and 6, the interaction energies of PE and PEO chains are illustrated versus the weight percent of functionalized factor. By these figures, the interaction strength between different functionalized SWCNTs with PE and PEO chains

Table 1 Comparison interaction energies of PE chain/different functionalized SWCNTs (in kcal/mol) with those of PE chain/unfunctionalized SWCNTs

Functionalization Type	Functionalizing factor weight percent					
	0 [37]	2	4	6	8	10
Mapped O	−497.31	−312.57	−247.3426	−425.55	−133.99	−621.74
Mapped OH	−497.31	−766.37	43.39	−645.51	−549.19	−740.44
Random mixed	−497.31	−394.2328	−573.6519	−266.9307	−452.8003	−553.9406

can be compared. Interestingly, for all of the functionalization types, the curves associated with PE and PEO polymers experience same trends. It is seen that for all of the cases, the PEO/nanotube interactions are more powerful than PE/nanotube interactions. This is true for mapped and random functionalized SWCNTs.

For the mapped OH functionalized SWCNTs, which is given in Fig. 4a, the minimum interaction energies associates with the weight percent of 4 %. Besides, the maximum interaction energies occur at 10 % weight percent. It is seen that increasing functionalization weight percent results in increasing the interaction energy for both chosen polymer chains. Figure 4b shows the interaction energies of polymer chains with random OH functionalized SWCNTs. The PE/SWCNT minimum and maximum interaction energies occur at two and six weight percentages for PE chain, respectively. The minimum and maximum values of PEO/SWCNT curve happens at 2 and 10 %, respectively.

For mapped O functionalized SWCNTs, Fig. 5a, the maximum and minimum interaction energies of both investigated chains occur at 10 and 8 %, respectively. Represented in Fig. 5b are the interaction chains of polymer chains with random O functionalized SWCNTs. It is seen that the curves are completely parallel. The maximum value occurs at 6 %. The

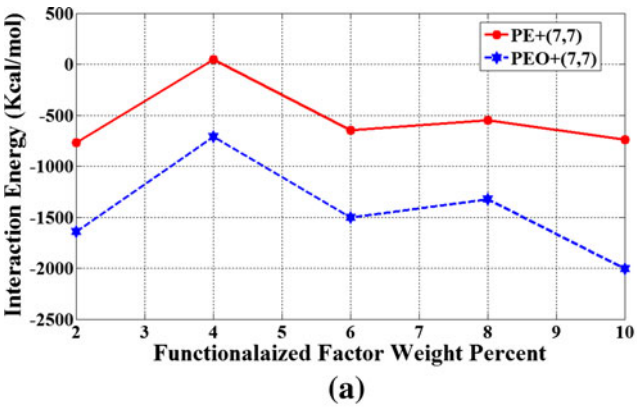

Fig. 4 Comparison of the interaction energies of (**a**) mapped and (**b**) random OH functionalized SWCNTs with PE and PEO polymer chains

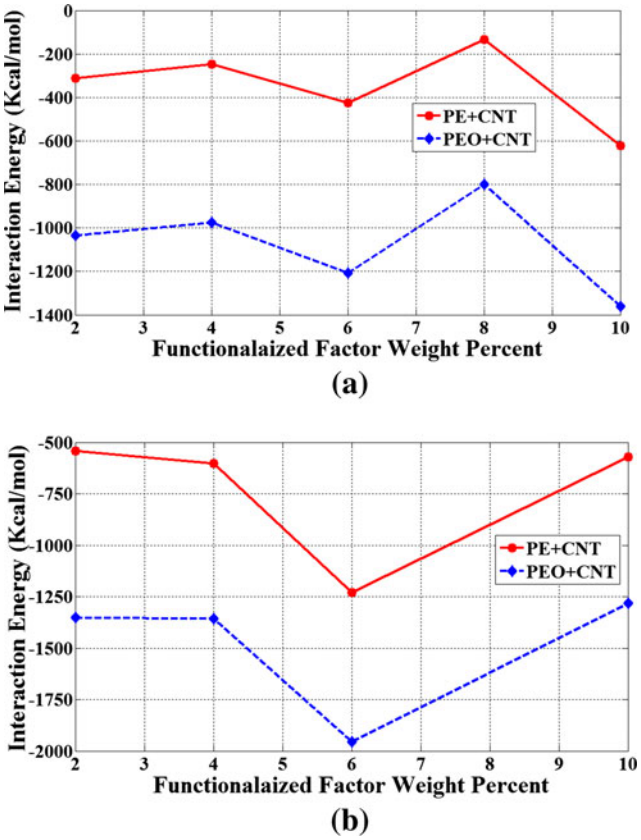

Fig. 5 Comparison of the interaction energies of (**a**) mapped and (**b**) random O functionalized SWCNTs with PE and PEO polymer chains

interaction energies of polymer chains with mixed functionalized SWCNTs are given in Fig. 6. An approximately same trend is observed for both chains. Besides, minimum interaction energy happens for 6 % weight percent. Moreover, the maximum interaction energy is for 10 % functionalization factor weight percent.

The effect of different functionalization factors are investigated in Fig. 7a, b for PE and PEO chains, respectively. It is seen that for both type of chains, the largest and smallest interaction energies of polymer relate to random oxygen and

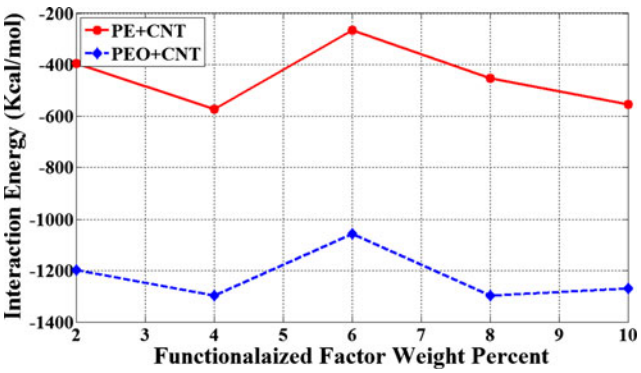

Fig. 6 Comparison of the interaction energies of random mixed functionalized SWCNTs with PE and PEO polymer chains

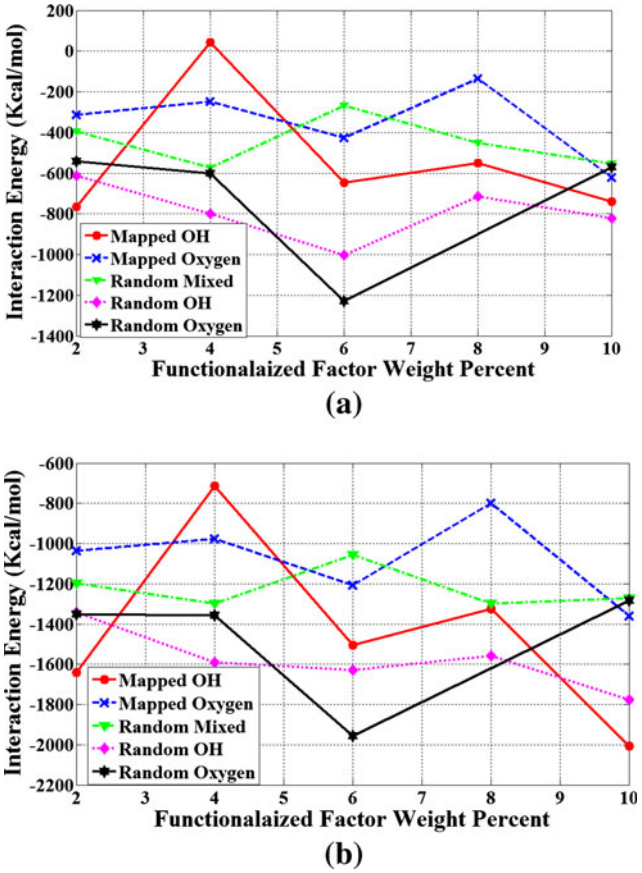

Fig. 7 The interaction energies of (**a**) PE and (**b**) PEO chains/different functionalized SWCNTs versus the functionalizing factor weight percent

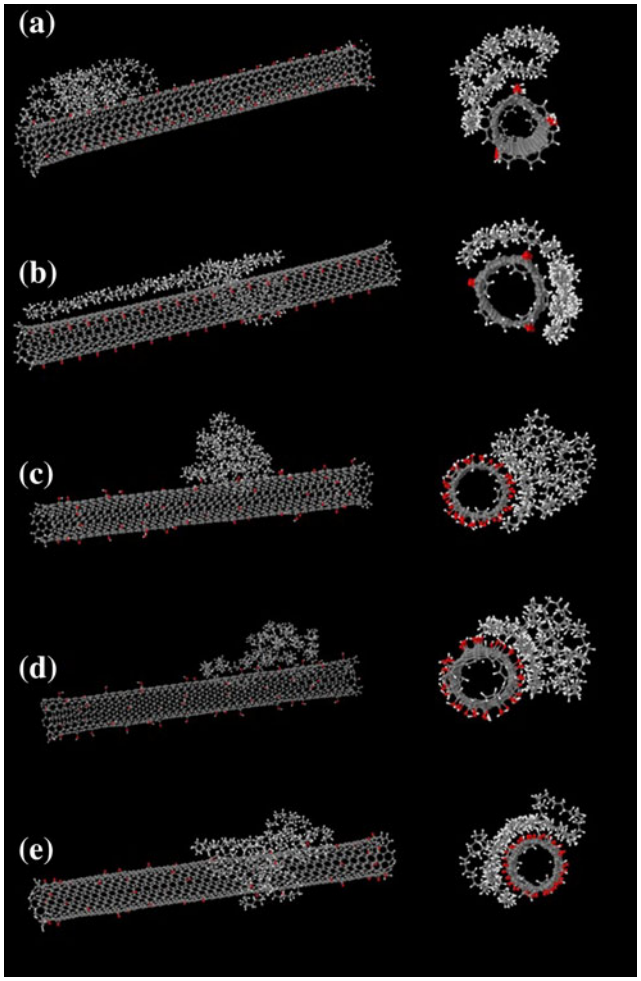

Fig. 8 Final conformations of PE chain at the side of functionalized SWCNTs with 6 % weight percent. **a** Mapped OH SWCNT. **b** Mapped O SWCNT. **c** Random mixed SWCNT. **d** Random OH SWCNT. **e** Random O SWCNT

mapped oxygen functionalized SWCNTs, respectively. The order of the interaction energies, from smallest to largest, is observed as random mapped O, random mixed, mapped OH, random OH, and random O. So, it can be concluded that random functionalization results in better reinforcement of SWCNTs by polymer chains. Besides, for random functionalization, O factors are better candidate to functionalize SWCNTs. However, mapped OH functionalized nanotubes have better interactions with polymer chains.

As it was previously mentioned, the time of 250 ps can be considered as the time at which the systems are relaxed. So, this time is considered as the time after which the adsorbed polymer chain configurations do not change. The represented snapshots are stable for a long period of time. In fact, after about 200 ps, the conformations of polymer chains do not change and only small translation and rotational motions happen. The final conformations of PE and PEO chains at the side of functionalized SWCNTs with 6 % weight percent are given in Figs. 8 and 9. Note that gray, white, and red colors are used to show C, H, and O atoms, respectively. It is seen that PE chains are adsorbed in more compact form than their PEO chains counterparts. Moreover, the PE/SWCNT interaction surfaces are higher than those of PEO/SWCNTs. For the mapped functionalized SWCNTs, the PE chains are adsorbed with approximately linear shapes. However, the PEO chains are contracted at the side of random functionalized SWCNTs. Considering PEO chains adsorbed on SWCNTs functionalized by different type of factors, one can conclude that rather than interaction with SWCNTs, the atoms of PEO chains prefer to interact with each other.

By comparing the conformations of PE chains adsorbed on the SWCNT surface for O and OH functionalized SWCNT, one can find that PE chains adsorbed on the both mapped and random O functionalized SWCNTs try to be in the maximum contact with SWCNT (Fig. 8b, e). In other words, more polymer atoms are in contact with SWCNT. However, the PE chains adsorbed on the counterpart OH SWCNTs have more contracted forms (Fig. 8a, d). So, one can conclude that for the PE/O functionalized SWCNTs, the governing interaction is a polymer/nanotube one. For PE/OH functionalized SWCNTs, the self-interaction of PE chains does not let the polymer

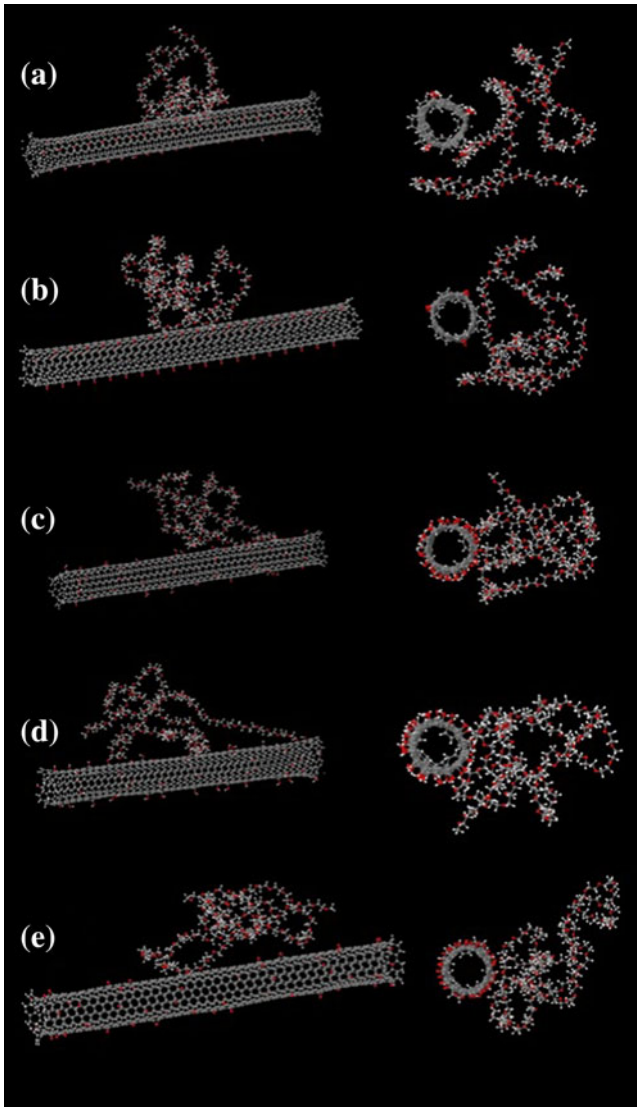

Fig. 9 Final conformations of PEO chain at the side of functionalized SWCNTs with 6 % weight percent. **a** Mapped OH SWCNT. **b** Mapped O SWCNT. **c** Random mixed SWCNT. **d** Random OH SWCNT, (**e**) Random O SWCNT

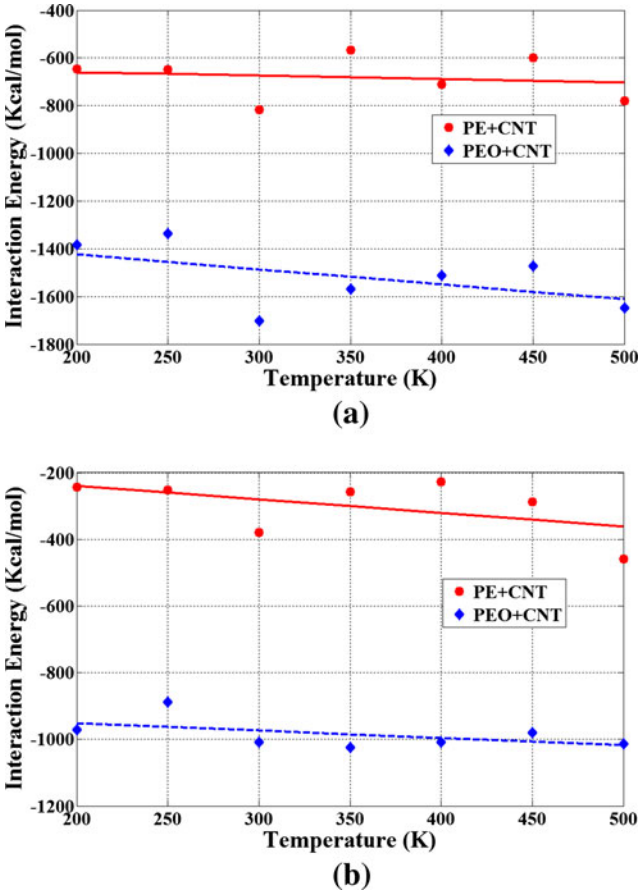

Fig. 10 Interaction energies of (**a**) mapped OH and (**b**) mapped O functionalized SWCNTs with PE and PEO polymer chains versus temperature

expand completely on the nanotube surface and be in full contact with it.

As it can be seen in Fig. 9, for the PEO chains, due to the large internal interactions of polymer atoms, the chains are not allowed to be in an efficient contact with SWCNT. This can be seen for both O and OH functionalized SWCNTs and mapped and random distribution patterns.

Comparing the results with the previous ones for PE chains adsorbed on the pristine SWCNTs [41], it can be concluded that adding functionalization factors on the nanotube surface results in PE chains with more contracted conformations. In other words, the PE chains have more extracted forms on the pristine nanotube surface. Comparing the results of PEO/functionalized SWCNT with the obtained results of pristine SWCNT [53], similar observations are obtained.

The effect of temperature on the interaction energy of PE and PEO/SWCNTs is investigated in Fig. 10. Two samples mapped O and mapped OH functionalized SWCNTs are considered here. The weigh percent of functionalization factor is 4 %. The range of 200–500 K with the step of 50 K is selected. For both of the factors and polymer chains, increasing temperature leads to increasing the interaction energy. It can be related to larger kinetic energies of chain atoms at higher temperatures. In fact, increasing temperature results in expansion of polymer chains. So, more atoms of chains can be exposed to the nanotubes. Hence, the interaction energy increases.

To study the effect of SWCNT diameter on the nanotube/polymer interaction, a (10,10) SWCNT with the same length is considered. Moreover, a (12,0) SWCNT is considered to investigate the effect of nanotube chirality. The radius of this SWCNT is approximately equal to the radius of (7,7) SWCNT. The interaction energies of these nanotubes functionalized by random mixed O and OH factors are given in Fig. 11. Comparing the curves, it is observed that the interaction energies of polymer/(10,10) SWCNT are larger than those

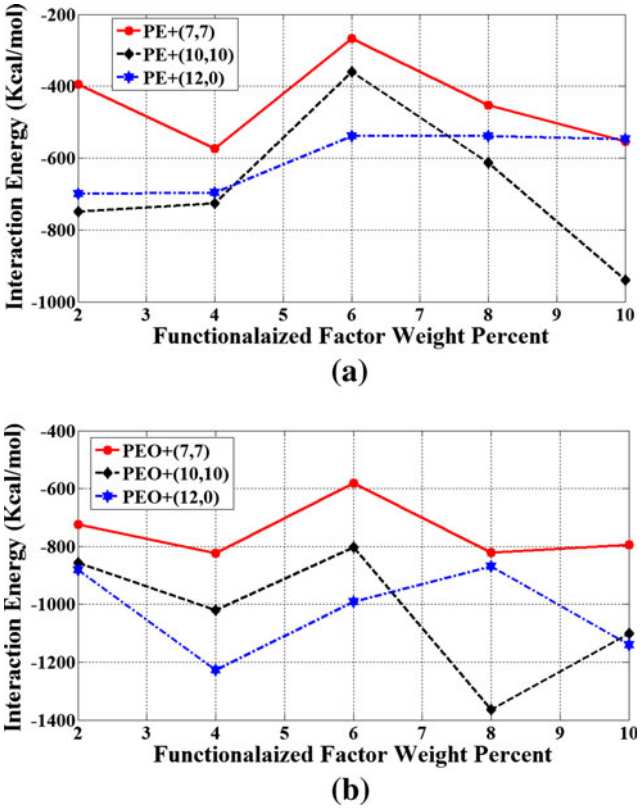

Fig. 11 Interaction energies of different random mixed functionalized SWCNTs with (**a**) PE and (**b**) PEO chains versus functionalized factor weight percent

of polymer/(7,7) SWCNT. It can be associated to the larger surface area of the nanotubes with larger diameters which increases the probability of the interaction between polymer and SWCNT atoms. Besides, the (12,0) SWCNT has larger interaction energies with polymer chains than (7,7) nanotube. So, one can conclude that zigzag nanotubes have better noncovalent interactions with polymer chains.

5 Concluding Remarks

The adsorption of PE and PEO chains on SWCNT surface was studied. MD simulations were used to do this. It was shown that the commonly used assumption for pure SWCNTs by which nanotubes are frozen during simulations cannot give reliable results for polymer/ functionalized SWCNT interactions. Besides, the PEO/SWCNT interaction energies are larger than those of PE/SWCNT. Comparing the results of different functionalization factors, random functionalization of SWCNTs with oxygen atoms gives the largest polymer/ SWCNT interaction energies. Finally, the final conformations of adsorbed chains were given. It was observed that PEO chains prefer to have less contracted forms compared to their PE counterparts.

References

1. R.F. Gibson, O.E. Ayorinde, Y.F. Wen, Compos. Sci. Technol. **67**, 1–28 (2007)
2. M.S. Dresselhaus, G. Dresselhaus, A. Jorio, Annu. Rev. Mater. Res. **34**, 247–278 (2004)
3. K. Saito, J. Nakamura, A. Natori, Phys. Rev. B **76**, 115409 (2007)
4. M. Cadek, J.N. Coleman, V. Barron, K. Hedicke, W.J. Blau, Appl. Phys. Lett. **81**, 5123–5125 (2002)
5. A.B. Dalton, S. Collins, E. Munoz, J.M. Razal, V.H. Ebron, J.P. Ferraris, J.N. Coleman, B.G. Kim, R.H. Baughman, Nature **423**, 703 (2003)
6. M. Cadek, J.N. Coleman, K.P. Ryan, V. Nicolosi, G. Bister, A. Fonseca, J.B. Nagy, K. Szostak, F. Beguin, W.J. Blau, Nano Lett. **4**, 353–356 (2004)
7. R. Ramasubramanjam, J. Chen, H. Liu, Appl. Phys. Lett. **83**, 2928 (2003)
8. J.K.W. Sandler, J.E. Kirk, I.A. Kinloch, M.S.P. Shaffer, A.H. Windle, Polymer **44**, 5893–5899 (2003)
9. C.Y. Wei, D. Srivastava, K. Cho, Nano Lett. **2**, 647–650 (2002)
10. J.Q. Pham, C.A. Mitchell, J.L. Bahr, J.M. Tour, R. Krishanamoorti, P.F. Green, J. Polym. Sci. B Polym. Phys. **41**, 3339–3345 (2003)
11. E. Kymakis, G.A. Amaratunga, Appl. Phys. Lett. **80**, 112–114 (2002)
12. I.D. Rosca, F. Watari, M. Uo, T. Akasaka, Carbon **43**, 3124–3131 (2005)
13. S. Osswald, M. Havel, Y. Gogotsi, J. Raman Spectrosc. **38**, 728–736 (2007)
14. V. Datsyuk, M. Kalyva, K. Papagelis, J. Parthenios, D. Tasis, A. Siokou, I. Kallitsis, C. Galiotis, Carbon **46**, 833–840 (2008)
15. S. Blazej, E. Borowiak-Palen, R.J. Kalenczuk, Mater. Charact. **61**, 185–191 (2010)
16. G.D. Sheng, D.D. Shao, X.M. Ren, X.Q. Wang, J.X. Li, Y.X. Chen, X.K. Wang, J. Hazard. Mater. **178**, 505–516 (2010)
17. K.A. Wepasnick, B.A. Smith, K.E. Schrote, H.K. Wilson, S.R. Diegelmann, D.H. Fairbrother, Carbon **49**, 24–36 (2011)
18. Y.C. Chiang, W.H. Lin, Y.C. Chang, Appl. Surf. Sci. **257**, 2401–2410 (2011)
19. N.F. Andrade, D.S.T. Martinez, A.J. Paula, J.V. Silveira, O.L. Alves, A.G. Souza Filho, J. Nanoparticle Res. **15**, 1–11 (2013)
20. P. Pandey, S. Mohanty, S.K. Nayak, High. Perform. Polym. **26**, 760–769 (2014)
21. V.V. Ivanovskaya, A.L. Ivanovskii, Russ. Chem. Rev. **80**, 727–749 (2011)
22. M. Baibarac, P. Gomez-Romero, J. Nanosci. Nanotechnol. **6**, 289–302 (2006)
23. Y.L. Zhao, J.F. Stoddart, Acc. Chem. Res. **42**, 1161–1171 (2009)
24. M.J. O'Connell, P. Boul, L.M. Ericson, C. Huffman, Y. Wang, E. Haroz, C. Kuper, J. Tour, K.D. Ausman, R.E. Smalley, Chem. Phys. Lett. **342**, 265–267 (2001)
25. D. Baskaran, J.W. Mays, M.S. Bratcher, Chem. Mater. **17**, 3389–3397 (2005)
26. A. Nish, J.Y. Hwang, J. Doig, R.J. Nicholas, Nat. Nanotechnol. **2**, 640–646 (2007)
27. H. Dohi, S. Kikuchi, S. Kuwahara, T. Sugai, H. Shinohara, Chem. Phys. Lett. **428**, 98–101 (2006)
28. Y.K. Kang, O.S. Lee, P. Deria, S.H. Kim, T.H. Park, D.A. Bonnell, J.G. Saven, M.J. Therien, Nano Lett. **9**, 1414–1418 (2009)
29. W. Yi, A. Malkovskiy, Y. Xu, X.Q. Wang, A.P. Sokolov, M.L. Colon, M.A. Meador, Y. Pang, Polymer **51**, 475–481 (2010)
30. M. Yang, V. Koutsos, M. Zaiser, J. Phys. Chem. B **109**, 10009–10014 (2005)
31. Y.H. Xie, A.K. Soh, Mater. Lett. **59**, 971–975 (2005)
32. W. Liu, C.L. Yang, Y.T. Zhu, M.S. Wang, J. Phys. Chem. C **112**, 1803–1811 (2008)

33. Q. Zheng, Q. Xue, K. Yan, L. Hao, Q. Li, X. Gao, J. Phys. Chem. C **111**, 4628–4635 (2007)
34. M. Bernardi, M. Giulianini, J.C. Grossman, ACS Nano **4**, 6599–6606 (2010)
35. M. Foroutan, A.T. Nasrabadi, J. Phys. Chem. B **114**, 5320–5326 (2010)
36. W.D. Cornell, P. Cieplak, C.I. Bayly, I.R. Gould, K.M. Merz, D.M. Ferguson, D.C. Spellmeyer, T. Fox, J.W. Caldwell, P.A. Kollman, J. Am. Chem. Soc. **117**, 5179–5197 (1995)
37. S.S. Tallury, M.A. Pasquinelli, J. Phys. Chem. B **114**, 9349–9355 (2010)
38. J. Pang, G. Xu, Y. Bai, S. Yuan, F. He, Y. Wang, H. Sun, A. Hao, Comput. Mater. Sci. **50**, 283–290 (2010)
39. Q. Wang, Phys. Lett. A **375**, 624–627 (2011)
40. Y. Zhang, J. Zhao, N. Wei, J. Jiang, Y. Gong, T. Rabczuk, Compos. Part B **45**, 1714–1721 (2013)
41. S. Rouhi, Y. Alizadeh, R. Ansari, Appl. Surf. Sci. **292**, 958–970 (2014)
42. S. Rouhi, Y. Alizadeh, R. Ansari, Fibers. Polym. **15**, 1123–1128 (2014)
43. J. Jilili, A. Abdurahman, O. Gülseren, U. Schwingenschlögl, Appl. Phys. Lett. **105**, 013103 (2014)
44. LAMMPS Molecular Dynamics Simulator. http://lammps.sandia.gov. (Accessed 1 March 2013).
45. S.J. Plimpton, J. Comput. Phys. **117**, 1–19 (1995)
46. M.P. Allen, D.J. Tildesley, *Computer Simulation of Liquids* (Clarendon, Oxford, 1987)
47. W.D. Cornell, P. Cieplak, C.I. Bayly, I.R. Gould, K.M. Merz, D.M. Ferguson, D.C. Spellmeyer, T. Fox, J.W. Caldwell, P.A. Kollman, J. Am. Chem. Soc. **117**, 5179–5197 (1995)
48. C. Grindon, S. Harris, T. Evans, K. Novik, P. Coveney, C. Laughton, Phil. Trans. R. Soc. A **362**, 1373–1386 (2004)
49. J. Wang, R.M. Wolf, J.W. Caldwell, P.A. Kollman, D.A. Case, J. Comput. Chem. **25**, 1157 (2004)
50. C. Caddeo, C. Melis, L. Colombo, A. Mattoni, J. Phys. Chem. C. **114**, 21109 (2010)
51. R. Ansari, S. Ajori, A. Ameri, Chem. Phys. Lett. **616–617**, 120 (2014)
52. R.R. Johnson, A.T.C. Johnson, M.L. Klein, Nano Lett. **8**, 69–75 (2008)
53. S. Rouhi, Y. Alizadeh, R. Ansari, Braz. J. Phys. **45**, 10–18 (2015)